J. exp. Biol. (1977), 69, 261–272
With 8 *figures*
Printed in Great Britain

CLAP AND FLING AERODYNAMICS – AN EXPERIMENTAL EVALUATION

By LEON BENNETT

Department of Applied Science, New York University, 26–36 Stuyvesant Street, New York, New York 10003

(*Received* 21 *February* 1977)

SUMMARY

The 'Clap and Fling' hypothesis, which describes augmentation of lift during the wingbeat of certain insects and birds, was evaluated experimentally in model form. Using induced velocity output as a lift index, and testing at a Reynolds number of roughly 83000, it was learned that:

1. The main 'Clap and Fling' aerodynamic effect consists of raising the lift output realized at the beginning of the stroke. After one chord of travel, 'Clap and Fling' effects are minor.
2. Considered over a complete stroke, 'Clap and Fling' lift output is limited to 1·15 times the lift output of an identical fixed incidence wing undergoing the same jump start trajectory.
3. 'Clap and Fling' output is limited by considerations of maximum circulation and circulation persistence. These limitations are not envisioned in current analyses.

INTRODUCTION

Weis-Fogh (1973, 1974, 1975) has suggested that a novel flight mechanism is employed by certain insects and birds to increase the amount of generated lift. The mechanism, termed 'Clap and Fling', has been subjected to analysis by Lighthill (1973) and Ellington (1974), both of whom confirmed the existence and power of the concept. The present paper describes an experimental, quantitative evaluation of the effect of 'Clap and Fling' upon the lift observed with model wings.

Readers who regard aerodynamics as an exact science may well ask why it is necessary to make an experimental study of a hypothesis that has received considerable analytical support. The answer is that aerodynamics contains numerous 'grey' areas of uncertainty, where complete analytical solutions are so difficult as to force the employment of a number of simplifying assumptions. The validity of the underlying assumptions can be tested only by appropriate experimental work. Examples of such assumptions in 'Clap and Fling' analyses are that viscous effects are generally unimportant, and that circulation is stable.

'Clap and Fling' is illustrated, in an insect, in Fig. 1 (taken from Weis-Fogh, 1975). In Fig. 1A the insect has arrived at one end of its wing stroke cycle: the two wings are held firmly together. The wings are then rotated about the trailing edge (Fig. 1B) so that the respective leading edges are flung apart. The wedge-shaped volume between the wings is filled with a flow of air (Fig. 1C) creating a circulation

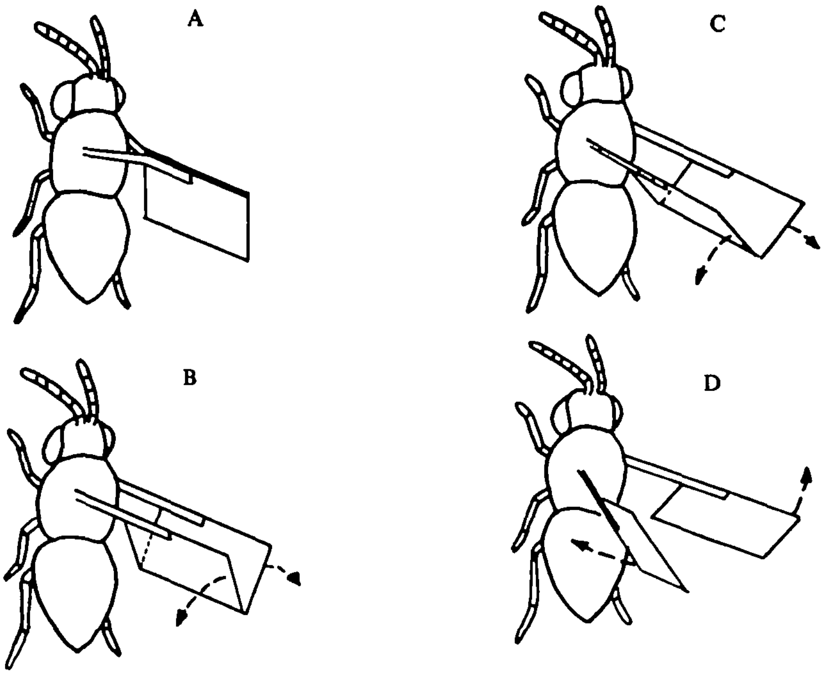

Fig. 1. Illustration of the 'Clap and Fling' concept, taken from Weis-Fogh (1975). See text for description of events.

which persists as the wings are separated at the trailing edge (Fig. 1D) by the stroke motion. The circulation is calculated to create lifting force equal to several times the lift derived without benefit of 'Clap and Fling'. The motion, restricted to only one end of the stroke cycle, is employed by certain species of insects and birds, such as the wasp *Encarsia formosa* and the Rock Dove. We shall assume that the above description of the motion is accurate.

An appropriate test for 'Clap and Fling' lift effectiveness is to compare measurements of lift output of a wing before and after removal of its partner. In real animals the surgery produces serious unbalanced forces with ensuing erratic behaviour. Fortunately, the motion to be tested is independent of subtle animal physiological characteristics, such as wing shape and stiffness, so mechanical modelling is suitable, and has been employed as follows.

METHODS AND MATERIALS

In essence, a single moving wing was directed along a two-dimensional trajectory similar to that specified by Weis-Fogh (1973, 1974, 1975). To simulate the presence of a clapping, partner wing, a virtual image plane (ground plane) was employed. By removing the virtual image plane, and repeating the trajectory exactly, a clapless (tare) run was produced. Finally, removing the virtual image plane permitted comparative runs with the wing driven at constant incidence. An evaluation of lift was obtained by measuring the induced velocity of that air under the moving wing. As certain of these techniques are novel, let us consider the procedure in detail. See Fig. 2.

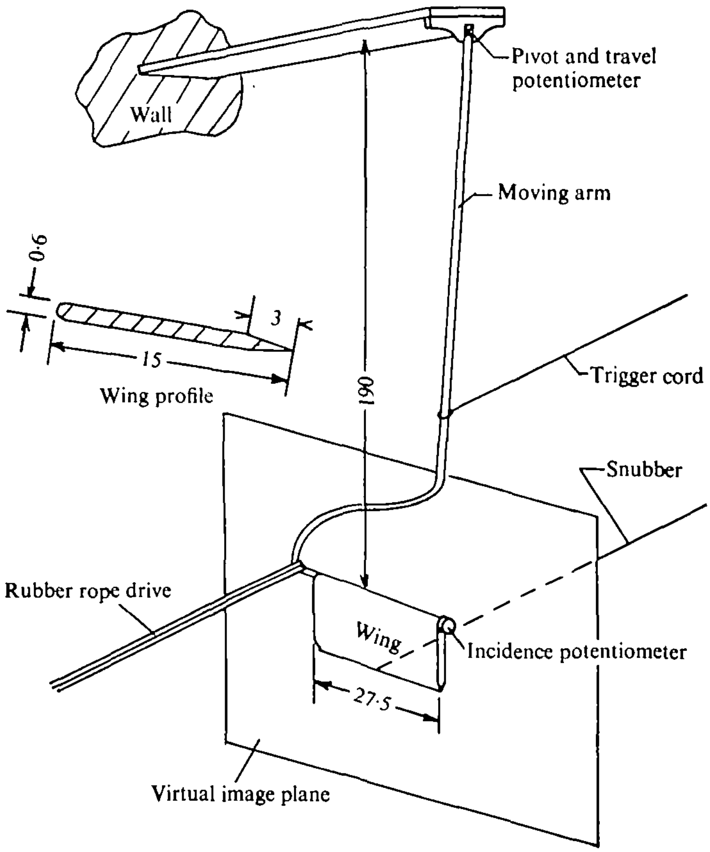

Fig. 2. Sketch of test apparatus and wing cross-section. All measurements in centimetres.

The wing is essentially a flat plate (4% thickness) with a rounded leading edge and sharp trailing edge. At its leading edge, the wing is mounted on bearings on a moving arm; rotation in incidence of the wing being arranged to occur about the origin of the leading edge. The arm has a considerable radius (190 cm). Its upper end rotates on a fixed bearing to carry the wing through its trajectory. The planform of the wing is rectangular (15 cm chord by 27·5 cm length).

The basic driving force comes from a rubber strand rope containing 16 strands of model aeroplane rubber (cross-section 6 × 1 mm). The free length of the rubber rope drive (roughly 45 cm) is approximately doubled when full tension (roughly 7 kg) is applied through the trigger cord. Upon release of the trigger cord, the rubber rope contracts sharply, driving the leading edge of the wing. Inertia and drag forces of the wing combine to resist the wing acceleration, resulting in a couple about the leading edge which acts to change the angle of incidence continuously. Larger velocities of incidence-change are obtained by use of a snubber line attached to the trailing edge of the wing. Through control of the leading edge rubber drive (changing the number of strands and/or initial extension) and similar control of the snubber rope, desired translational and incidence velocities may be obtained.

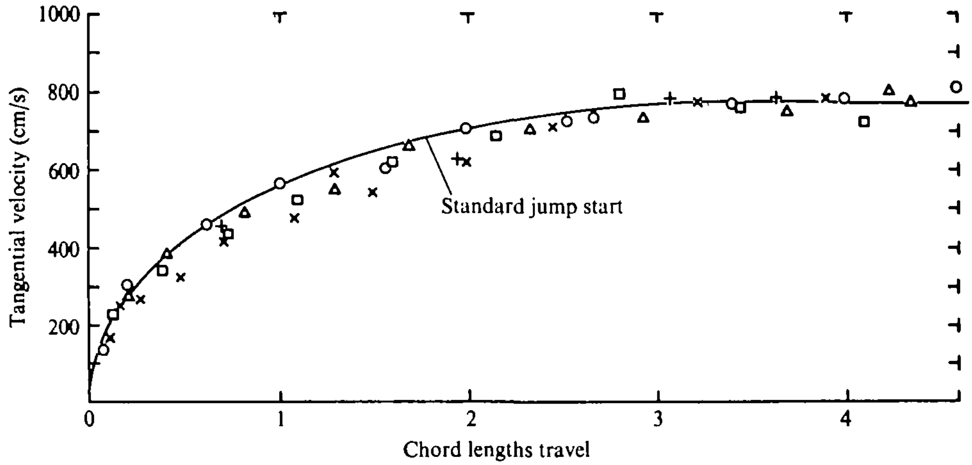

Fig. 3. Velocity history of jump start. All results given in this study employ the jump start. Different runs are represented by different symbols. These symbols represent the same runs in this figure as in Figs. 4, 6 and 7.

To measure translational and incidence change velocities, potentiometers were mounted to the upper and lower ends of the moving arm. Potentiometer readings, calibrated to reflect angular position, were continuously recorded on a suitable oscillograph (CEC 5-124) equipped with galvanometers offering a flat frequency response up to 350 Hz. Velocities were obtained by graphically differentiating the position trace with respect to time in the usual fashion. Typical tangential rate changes are given in Fig. 3.

The stationary image plane is a classic tool of experimental aerodynamics, truly representing all aspects of opposing-twin flow events when used in conjunction with either of the set partners. While most aeronautical engineering undergraduate texts carry some description of the phenomenon, the treatment of this subject by von Karman and Burgers (1935) is particularly lucid and thorough. Frequent practical use is made of a virtual image plane to simulate an opposing potential flow occurrence; in particular, wind-tunnel workers deal with such boundary effects as an everyday matter. The virtual image plane employed in these experiments was made of large dimensions (122 × 61 cm) and quite thick (2 cm) to permit the wing to be pressed firmly against the wall without wall deflexion and subsequent reverberation. The snubber line passed through a small hole in the wall.

To evaluate lift, the induced velocity created by the moving wing was monitored. Induced velocity measurements has the advantage over the usual force-measuring apparatus of being insensitive to inertial loading of any form. When dealing with powerful transients, as is the case here, the unwanted inertial loads can be orders of magnitude larger than the aerodynamic loads. While in principle such inertial loads can be tared out of a force measuring system, the taring process is not simple: for example, the entire assembly has to be operated in a vacuum to separate aerodynamic and inertial loads.

If the induced velocity component v_1 is defined as that velocity directed opposite to a hovering lift force L, the incremental lift dL created at a small sample volume experiencing a through flow dQ is $dL = Av_1\, dQ$, where A is a suitable constant

This expression is a classic momentum relationship. The flow term dQ is equal to $C(v_1 +\!\!\!\!\rightarrow v_2 +\!\!\!\!\rightarrow v_3)$, where the v terms represent orthogonal components of velocity within the sample volume and C another suitable constant reflecting sample volume cross-sectional area and fluid density considerations. Thus dL is equal to $Ev_1 \times (v_1 +\!\!\!\!\rightarrow v_2 +\!\!\!\!\rightarrow v_3)$, where E is a suitable constant or, in words, the lift is proportional to the product of the induced velocity component v_1 and the resultant velocity through the test zone.

The component v_3 will be defined as the flow induced in a spanwise direction. As all experimental readings are taken along the wing centre-line, v_3 is necessarily zero by considerations of symmetry. The component v_2, or that existing in a fore-and-aft sense, can be separated from v_1 in the data by a tedious procedure given elsewhere (Bennett, 1970). Noting that in the course of 'Clap and Fling' tests v_2 proved less than 15 % of v_1, the following approximation has been employed:

$$v_1 = (v_1 +\!\!\!\!\rightarrow v_2)$$

and

$$dL \propto (v_1 +\!\!\!\!\rightarrow v_2)^2.$$

(In what follows the term $(v_1 +\!\!\!\!\rightarrow v_2)$ shall be referred to as the induced velocity.) Thus in this analysis the generated lift is viewed as proportional to the induced velocity squared. Such an approximation is in error by roughly 1 %, as can be shown thus:

$$\sqrt{(100\%)^2+(15\%)^2} = 101\%.$$

As noted, induced velocity readings are taken only along the centre-line of the moving aerofoil to avoid v_3 considerations. There is a drawback to this arrangement: it is impossible to investigate the entire flow field to arrive at $\int dL$, so we are limited to measurements of incremental lift observed at fixed spaced stations along the flight path. While such measurements are quantitative, they are useful primarily for purposes of comparison, for example, 'Clap and Fling' versus a constant incidence condition. Such comparisons, based on local induced velocity, form the bulk of the present results.

Induced velocity was monitored with a standard hot-wire anemometer (Flow Corp., Model CT-A2) equipped with a thick probe wire offering a flat response up to 2500 Hz. Presentation was in analogue form through the same oscillograph and galvanometers given above. Calibration was obtained in the conventional fashion with a miniature wind tunnel and micromanometer attached to a pitot tube.

The entire argument given above can be summarized (with some loss of sophistication) as follows: lift force equals the rate of flow of downward momentum. If the induced velocity is very nearly downwards, the rate of flow of momentum is proportional to the square of induced velocity. Thus, by comparing the magnitudes of experimentally derived induced velocities after squaring, the relative lifting forces are determined. By always employing the same wing and identical wing tangential velocities, the parameters under test are reduced to (i) incidence, and rate of change of incidence, (ii) the presence or absence of a partner virtual wing.

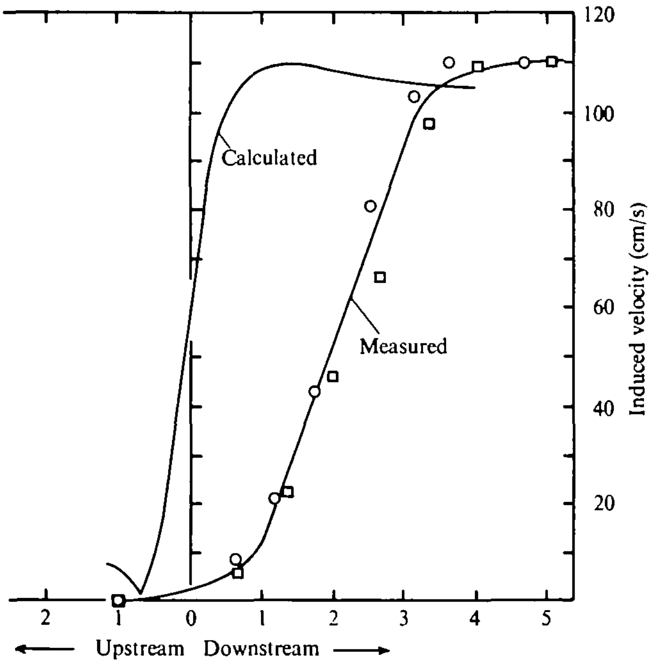

Fig. 4. Induced velocity generated by the test wing at constant incidence after a standard jump start. The abscissa gives the instantaneous location of the wing, in chord lengths, with respect to a fixed hot wire sensor positioned three chord lengths upstream of the start. The ordinate represents the induced velocity sensed at the fixed hot-wire sensor.

RESULTS

Conventional aerodynamics of the wing

To test the various assumptions and approximations employed in this work, some runs were perfoımed with the wing driven at constant incidence and essentially constant tangential velocity. The latter condition corresponds roughly to the steady-state condition in which the induced velocity field is everywhere known and readily calculated through use of the classic horseshoe vortex concept. By comparing experimental and analytical results for this simple case (Fig. 4), we gain a sense of both the accuracy and the limitations of the experimental approach.

In this case, all induced velocity readings were taken at a single station located sufficiently far upstream of the start (three chords) that, despite the jump start (Fig. 3), essentially steady-state conditions existed by the time the fixed-incidence wing (14·5°) passed over the test station. Each plotted point (Fig. 4) has as its abscissa the instantaneous wing location with respect to the test station. The ordinate value is the corresponding induced velocity. Two independently obtained experimental runs, reflecting superficially identical tests, are shown to supply a sense of typical scatter encountered in this work. The computed induced velocity values were obtained from Biot-Savart law considerations, taken together with the Zhukovsky theorem; the lift coefficient was taken as 2π times the angle of incidence. Thus, only classic inviscid concepts were applied.

Note that in Fig. 4 the predicted and measured maximum values of induced velocity are in good agreement. There is a large time lag between the predicte

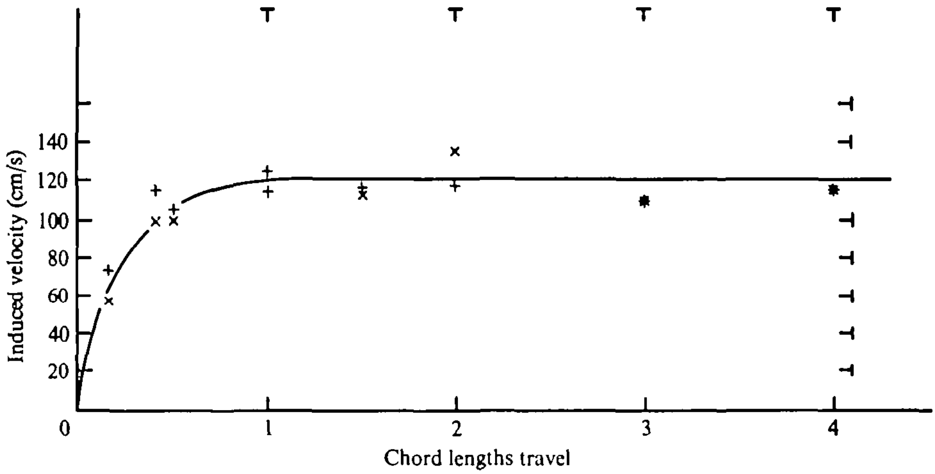

Fig. 5. Induced velocity peak values (of the two runs shown in Fig. 4) as a function of travel for the constant incidence condition. The peak values of Fig. 4 are represented by coincident points of 110 cm/s magnitude at 3 chord lengths of travel.

arrival and the measured arrival of the induced velocity, corresponding to roughly two chord lengths of travel or 0·04 s, but fortunately the 'Clap and Fling' lift assessment requires only local maximum induced velocity values; time of arrival does not enter into our calculations (see Methods and Materials). In other words, the single experimental result describing generated lift to be abstracted from Fig. 4 is the maximum value of induced velocity, roughly 110 cm/s. Using this value, we arrive at the lift output per cm² of test zone swept area,

$$dL = E \times (110)^3,$$

a result essentially identical to that obtained from purely theoretical inviscid considerations. Thus we conclude that the lift based induced velocity results are in accord with inviscid predictions and that the experimental apparatus is satisfactory for our purposes.

By getting local maximum induced velocity results along the wing trajectory, lift may be determined as a function of travel from the starting point. Fig. 5 gives such a presentation for fixed incidence results. Each plotted point is the result of a separate run on which a transient wave of induced velocity swept over the given station, located a known distance from the starting point. In other words, the lift output was sensed at each station, not as a continuous phenomenon, but rather as the short-term peak of a passing pulse. For example, all the results of Fig. 4 are represented, in this procedure, by a pair of coincident points at the three chord length travel position. This form of data gathering and presentation is particularly useful in dealing with unsteady output.

Should the time lag, already noted above, cause some lessening of the peak value of induced velocity owing to a viscous smoothing action, we will be attributing less than the proper value of lift to the wing. So long as we compare the lift values gathered under identical test conditions, the relative effect of such an attenuation is believed small.

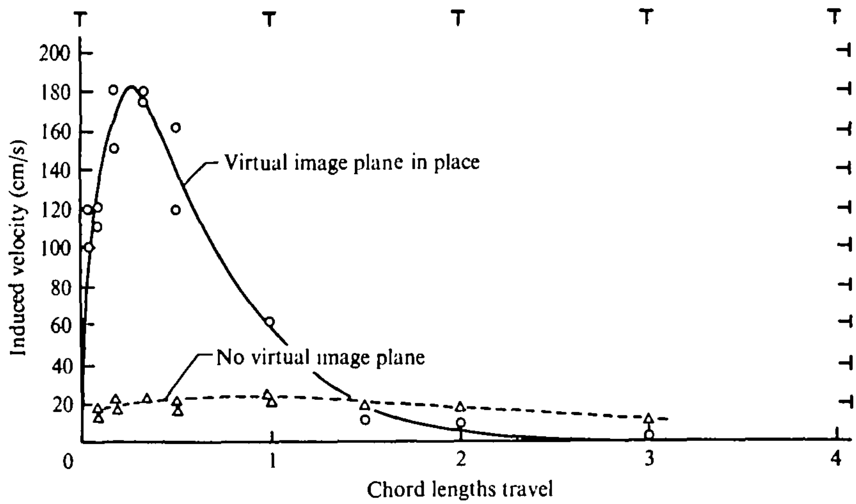

Fig. 6. 'Clap and Fling' induced velocity peak values as a function of travel. Maximum value of rate of change of incidence (w) equals 31 rad/s. The particular 'Clap and Fling' output shown (virtual image plane in place) is the maximum of all results.

In the fixed-incidence case, a steady lift output is anticipated once the period of initial acceleration and circulation growth is complete. The results of Fig. 5 support these expectations; after roughly one chord of travel, the induced velocity output becomes stable.

'Clap and Fling' results comparable to the fixed incidence results of Fig. 5 are given in the upper portion of Fig. 6. Two separate conditions are shown: one in which a virtual image plane is employed to completely simulate 'Clap and Fling', and a second in which the virtual image plane is removed. In both cases the peak value of incidence rate change is 31 rad/s, a value reached at about 0·8 chord of translation. Jump-start tangential velocities may be obtained from Fig. 3. The particular conditions and results given in Fig. 6 reflect the maximum output of all the 'Clap and Fling' tests.

The initial values of generated induced velocity (Fig. 6) are far greater when the virtual image plane is in place. After one half chord the difference diminishes steadily until, at about $1\frac{1}{2}$ chords of travel, a cross-over occurs such that 'Clap and Fling' output is smaller than 'clapless' output. Note further, by comparing Figs. 5 and 6, that after one chord of travel the output of the fixed incidence wing is higher than either the 'Clap and Fling' or 'clapless' configuration. Thus our results would indicate 'Clap and Fling' to be beneficial in terms of lift output; however, such benefits are of short duration.

In an attempt to increase the persistence of 'Clap and Fling' lift output, the peak value of incidence rate was increased to 69 rad/s with the results given in Fig. 7. The effect of increasing the incidence rate change was to decrease both the overall lift output and the persistence. Further, the data scatter was greatly worsened, suggesting that the wing was operating in a stalled condition.

To determine the lift gain over the entire cycle through use of 'Clap and Fling', we may reason as follows. First, the induced velocity values of Fig. 6 are the largest value

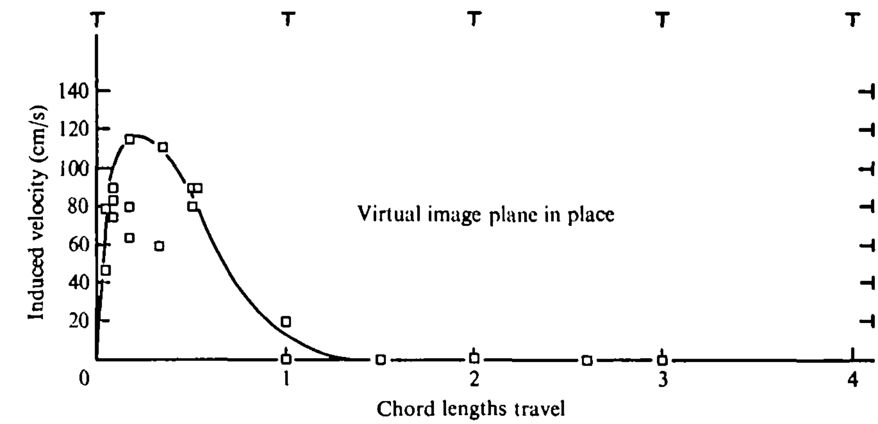

Fig. 7. 'Clap and Fling' induced velocity peak values as a function of travel. Maximum value of rate of change of incidence (ω) is 69 rad/s.

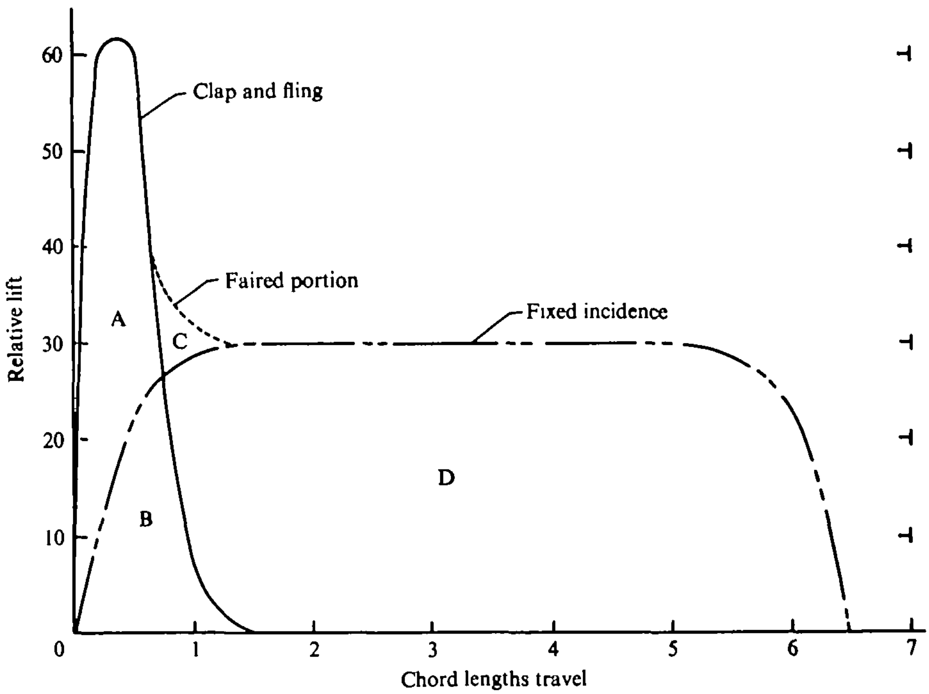

Fig. 8. Incremental lift experienced at the test zone as a function of travel. The lift values while relative only, are directly proportional to absolute lift. The areas marked A–D are employed to determine the performance of 'Clap and Fling' as compared to the fixed incidence condition.

capable of realization through 'Clap and Fling' for the standard wing and jump-start condition. Numerous tests (not given) at various conditions of incidence and incidence rate velocity all produced outputs smaller than those given by the particular test conditions reflected in Fig. 6. For example, see Fig. 7. Therefore the maximum lift possible is proportional to the square of induced velocity values taken from Fig. 6. To extend the travel base line to a value suited to a typical flying animal,

$6\frac{1}{2}$ chord lengths of traverse (a single downstroke) was employed as the abscissa. On this base, both the lift output of the 'Clap and Fling' optimum run and comparable values of the constant incidence run were constructed. See Fig. 8. Noting that the benefits from 'Clap and Fling' end in less than a chord length of travel, we may credit the animal with sufficient ability to switch from 'Clap and Fling' to constant incidence lift at about the one chord travel point. The switch is shown by the faired portion of the output curve. By comparing the area under the composite curve ('Clap and Fling' plus faired portion) to the area under the constant incidence curve, we have a measure of improvement in lift values over the entire cycle gained through use of 'Clap and Fling'. In terms of Fig. 8, the improvement may be measured by taking the ratio of areas (A+C)/(B+D). The calculated percent gain in lift is 15%.

DISCUSSION

The test results indicate 'Clap and Fling' lift benefits to be real, although modest. Two separate limitations exist concerning the lift intensity actually realized. These are limitations of magnitude and persistence.

The magnitude of circulation developed under 'Clap and Fling' has been given by Weis-Fogh (1974) as

$$\Gamma = \Omega c^2 g(a),$$

where Γ is the circulation, Ω is the angular rate of change of incidence, c is the chord and $g(a)$ is a function of the angle of leading edge wedge opening prior to trailing edge motion. Fortunately $g(a)$ is relatively insensitive to precise values of wedge angle and for our purposes we may substitute a constant value; say 0·7, as obtained from Weis-Fogh (1974, fig. 11). Noting that Ω is exactly twice the value of incidence rate change experimental values developed in this work, owing to the effect of the virtual image plane, we have in our case

$$\Gamma = 1{\cdot}4\omega c^2,$$

where ω is the experimental incidence rate change. This expression is open ended and without limit; larger values of ω should always lead to larger values of circulation and thereby to larger values of lift.

In practice we find that limits to useful values of circulation do exist. Substituting test condition values employed in the maximum output run (Fig. 6) into the above expression, $\Gamma = 9000\ \mathrm{cm^2/s}$, a circulation result close to that developed by the same wing operating at steady state maximum lift coefficient conditions ($\Gamma = 9120\ \mathrm{cm^2/s}$). Attempting to create a larger circulation value, via 'Clap and Fling' type incidence rate changes, actually lowers the amount of lift produced (Fig. 7) and signs of separation (stall) are clearly reflected in the induced velocity data. Thus it would appear possible that 'Clap and Fling' circulation is limited to the same maximum values derived without 'Clap and Fling'. The virtue of 'Clap and Fling' circulation is one of early production in the wing-beat cycle, when conventionally derived circulation is small.

As concerns persistence, Weis-Fogh (1973) stated that 'considerable circulations around the two wings *would* remain at the end of the fling' and Ellington (1974) performed calculations indicating some residual increase of circulation to persist through four chord lengths of travel. The above results do not support these expectations. The circulation gain drops quickly as the wing moves from 'Clap' into 'Fling'. Within a travel of $1\frac{1}{2}$ chords (Fig. 6) all circulation gained through the 'Clap' is gone. At the end of one chord length of travel (Fig. 8) a conventional wing operating at optimum fixed incidence out-performs any tested 'Clap and Fling' configuration. It appears that the persistence of any circulation gain through 'Clap and Fling' is quite short in duration and limited to roughly the first chord of travel.

The reasons for the limits on 'Clap and Fling' circulation magnitude and circulation persistence were only partially revealed in this work. While the evidence does indicate that stall (severe separation of airflow) is a limiting factor in achieving large values of circulation, the reason for the short persistence of circulation is less apparent. I can speculate as follows. 'Clap and Fling' is a mechanism through which a 'forced' circulation is developed in an unstable manner. The instability is particularly marked in a period of circulation reduction, where instead of the usual exponential decay trend, total collapse ensues. The stability problem attendant upon a decreasing 'forced' circulation is one well known in aerodynamics. For example, the experimental work of Halfman (1951) demonstrates a similar form of circulation collapse when wings are oscillated beyond incidence attitudes corresponding to maximum stable steady state values. Stall and circulation stability considerations are difficult analytical areas in which the inviscid approach is severely limited. Therefore the existing analyses of 'Clap and Fling' are insensitive to the presence of the problem.

Since circulation stability is the key consideration in practical employment of 'Clap and Fling', it is possible that the stability characteristics of the particular aerofoil and wing planform configuration employed in these tests influenced the results. However, what we know of circulation stability indicates the design tested to be among the best suited for circulation stability purposes. Indeed the thin flat plate with a rounded leading edge and a low aspect ratio is taken from traditional tail-surface design of light aircraft, where it is used because of its proven circulation stability characteristics. We have no reason to assume superior characteristics on the part of insects and birds.

Given the twin limits upon circulation magnitude and endurance it becomes evident that 'Clap and Fling' can bring only a modest increase to overall lift output. To apply these results to flying animals, note should be taken of the scale (Reynolds number or *Re*) at which these tests were conducted, roughly 83000. Such a value is far removed from the *Re* of insects proposed to employ 'Clap and Fling', e.g. *Encarsia formosa* has an *Re* of less than 20 (Weis-Fogh, 1975). Lacking test data at a suitably low *Re*, we note that 'Clap and Fling' is inviscid in concept and that all known inviscid circulation schemes perform rather poorly as the domain becomes viscous, i.e. as *Re* becomes small. Therefore at low *Re*, say a value of 20, performance gain due to 'Clap and Fling' action will be considerably lower than the 15% observed in this work. Specifically, we can anticipate lower maximum circulation values owing to limits on rate of rise of circulation in a highly viscous medium. We can also anticipate still smaller values of persistence. It can thus be conjectured that no significant gain in overall lift output will be apparent in the case of small insects via 'Clap and Fling'. In the case of large birds a modest but significant improvement in performance appears possible.

The very modesty of the overall 'Clap and Fling' lift gain raises a question as the purpose of any animal employing the concept. Perhaps additional lift is not the goal. It would seem at least equally likely that the objective is one of creating a nose-down moment by displacing the centre of lift in a rearwards direction. Helicopters leaving the hovering position to assume a forward flight attitude achieve the necessary tilting of the tip plane by increasing the lift developed at the rearmost blade. This effect is produced by 'Clap and Fling'. Thus animals such as rock dove that are reputed to employ a single 'clap' to initiate forward flight may well be tilting their flapping plane into an appropriate attitude rather than seeking to augment total lift.

Appreciation is expressed to graduate students Greg Kiviat and Yan Chan for data gathering and reducing efforts and to the National Science Foundation (NSF-ENG74-04873) for sponsorship.

REFERENCES

BENNETT, L. (1970). Insect flight: lift and rate of change of incidence, *Science, N.Y.* **167**, 177–9.

ELLINGTON, C. P. (1974). In *Swimming and Flying in Nature*, vol. 2 (ed. Y. T. Wu, C. J. Brokaw and C. Brennen), pp. 783–96. Plenum Press.

HALFMAN, R. L. (1951). Experimental aerodynamic derivatives of a sinusoidally oscillating airfoil in two dimensional flow. *NACA Tech. Rep.*, no. 1108.

VON KARMAN, T. & BURGERS, J. M. (1935). In *Aerodynamic Theory*, vol. II (ed. W. F. Durand), pp. 236–47. Julius Springer; reprinted 1963, London: Dover.

LIGHTHILL, M. J. (1973). On the Weis-Fogh mechanism of lift generation. *J. Fluid Mech.* **60**, 1–17.

WEIS-FOGH, T. (1973). Quick estimates of flight fitness in hovering animals, including novel mechanisms for lift production. *J. exp. Biol.* **59**, 169–230.

WEIS-FOGH, T. (1974). In *Swimming and Flying in Nature*, vol. 2 (ed. Y. T. Wu, C. J. Brokaw and C. Brennen), pp. 729–62. Plenum Press.

WEIS-FOGH, T. (1975). Unusual mechanisms for the generation of lift in flying animals. *Scient. Am.* **233**, 80–7.